Gastric Cancer (2021) 24:624–639
https://doi.org/10.1007/s10120-020-01154-5

ORIGINAL ARTICLE

A multi-mode Wnt- and stemness-regulatory module dictated by FOXM1 and ASPM isoform I in gastric cancer

Chung-Chi Hsu[1] · Wen-Ying Liao[2] · Kwang-Yu Chang[3] · Tze-Sian Chan[2,4,5,6] · Po-Jui Huang[2,5,6] · Chun-Ting Chiang[7] · Yan-Shen Shan[8] · Lin-Hsin Cheng[2] · Tai-Yan Liao[2] · Kelvin K. Tsai[2,3,5,6,9,10]

Received: 26 September 2020 / Accepted: 24 December 2020 / Published online: 29 January 2021

Abstract

Background Gastric cancer (GC) is the third leading cause of cancer mortality globally and a molecularly heterogeneous disease. Identifying the driver pathways in GC progression is crucial to improving the clinical outcome. Recent studies identified ASPM (abnormal spindle-like microcephaly-associated) and FOXM1 (Forkhead box protein M1) as novel Wnt and cancer stem cell (CSC) regulators; their pathogenetic roles and potential crosstalks in GC remain unclarified.

Methods The expression patterns of ASPM isoforms and FOXM1 were profiled in normal gastric epithelial and GC tissues. The functional roles of ASPM and FOXM1 in Wnt activity, cancer stemness and GC progression, and the underlying signaling processes were investigated.

Results Approximately one third of GC cells upregulate the expression of ASPM isoform I (ASPMiI) in their cytoplasm; the tumors with a high ASPMiI positive score ($\geq 10\%$) are associated with a poor prognosis of the patients. Mechanistically, the molecular interplay among FOXM1, ASPMiI and DVL3 was found to converge on β-catenin to control the Wnt activity and the stemness property of GC cells. This multi-mode Wnt-regulatory module serves to reinforce Wnt signals in CSCs by transcriptional regulation (FOXM1–ASPM), protein–protein interactions (ASPMiI–DVL3–β-catenin), and nuclear translocation (FOXM1–β-catenin).

Conclusions This study illuminates a novel Wnt- and stemness-regulatory mechanism in GC cells and identifies a novel subset of FOXM1^{high}ASPMiI^{high} GC with potential to guide Wnt- and stemness-related diagnostics and therapies.

Keywords FOXM1 · ASPM · Wnt · Gastric cancer · Stemness

Chung-Chi Hsu, Wen-Ying Liao contributed equally to this work.

✉ Kelvin K. Tsai
tsaik@tmu.edu.tw

[1] School of Medicine, College of Medicine, I-Shou University, Kaohsiung City 824410, Taiwan

[2] Laboratory of Advanced Molecular Therapeutics, Graduate Institute of Clinical Medicine, College of Medicine, Taipei Medical University, 250 Wuxing St., Xinyi Dist., Taipei City 110301, Taiwan

[3] National Institute of Cancer Research, National Health Research Institutes (NHRIs), Tainan City 704016, Taiwan

[4] School of Medicine, College of Medicine, Taipei Medical University, Taipei City 110301, Taiwan

[5] Division of Gastroenterology, Wan Fang Hospital, Taipei Medical University, Taipei City 110301, Taiwan

[6] Integrative Therapy Center for Gastroenterological Cancers, Wan Fang Hospital, Taipei Medical University, Taipei City 110301, Taiwan

[7] Department of Pathology, National Cheng-Kung University Hospital, Tainan City 704302, Taiwan

[8] Department of Surgery, National Cheng-Kung University Hospital, Tainan City 704302, Taiwan

[9] TMU Research Center of Cancer Translational Medicine, Taipei Medical University, Taipei City 110301, Taiwan

[10] TMU and Affiliated Hospitals Pancreatic Cancer Group, Taipei Medical University, Taipei City 110301, Taiwan

Introduction

Notwithstanding the gradual decline in the incidence of gastric cancer (GC), it remains the fifth most common cancer and the third leading cause of cancer deaths worldwide [1]. Despite the advances in chemotherapy and the anti-vascular endothelial growth factor receptor 2 antibody ramucirumab, the majority of patients with advanced GC continue to have disease progression following treatments [2]. Recently, immune checkpoint inhibitors have demonstrated clinical efficacy with an objective response rate of 11–12% in patients with advanced GC [3, 4]. However, the survival benefit is small albeit statistically significant and the treatment efficacy is limited to a small subset of patients [3, 5]. Establishing clinically relevant and biology-informed classification systems in GC and the associated biomarkers to facilitate the development of novel molecularly targeted and rational therapies remains an urgent and highly unmet clinical need.

The Wnt-regulated self-renewal processes in epithelial tissues are frequently hijacked by cancer cells to facilitate malignant progression [6–9]. Dysregulated Wnt pathway activity plays a crucial role in sustaining the phenotypes in stem-like cancer cells or "cancer stem cells (CSC)" [6, 8, 9]. In GC, approximately 10–30% of the tumors display deregulated Wnt signaling by developing genetic lesions affecting multiple levels of the Wnt signaling pathway [10, 11]. ASPM (abnormal spindle-like microcephaly associated) is a centrosomal protein that regulates neurogenesis and brain size and is also widely expressed in a variety of tissues [12, 13]. ASPM expression is up-regulated in various malignant tumors [13–16], wherein it serves as an oncoprotein and a positive regulator of Wnt-β-catenin signaling and cancer stemness [17–20]. Interestingly, ASPM has been shown to express in the scattered stem/progenitor cells existing in the isthmus zone of gastric oxyntic mucosa, and its expression is up-regulated in GC cells [21]. The precise pathogenetic role of ASPM in GC and the underpinning mechanistic basis have yet been rigorously investigated.

FOXM1 (Forkhead box protein M1) is a member of the Forkhead transcription factors that regulate the expression of genes involved in cell cycle regulation, development, organ regeneration, and tumorigenesis [22–26]. Aside from serving as a transcription factor, recent studies unraveled the pleiotropic functions of FOXM1 such as its effect to facilitate the nuclear translocation of β-catenin in glioma and leukemia cells [27, 28]. Furthermore, FOXM1 has also been found to regulates CSCs in pancreatic cancer, and its expression is upregulated in GC and poor prognostic [29, 30]. Given that both ASPM and FOXM1 have been shown to regulate the Wnt/β-catenin signaling pathway and cancer stemness, we set out to determine their potential molecular and epistatic relationships in GC cells with the goal of identifying novel pathomechanisms underlying the aggressiveness of human GC, which may unlock strategies to improve the prognostic classification of patients as well as to develop novel rational therapies for advanced and aggressive GC.

Materials and methods

Bioinformatics analysis

The RNA sequencing transcript level of *ASPM* and *FOXM1* in GC and normal gastric tissues in The Cancer Genome Atlas (TCGA) was interrogated from the GEPIA database (http://gepia.cancer-pku.cn). The survival data of 593 GC patients stratified based on the *ASPM* (Affymetrix ID: 219918_s_at) and the *FOXM1* (Affymetrix ID: 202580_x_at) transcript level were downloaded from KM Plotter (http://kmplot.com/analysis/index.php?p=service&cancer=gastric). The survival data of 352 GC patients in TCGA were downloaded from SurvExpress (http://bioinformatica.mty.itesm.mx:8080/Biomatec/SurvivaX.jsp).

Immunohistochemistry (IHC) and immunofluorescence (IF) analysis

The tissue microarrays (TMA) of 59 GC and the matched normal tissues were obtained from SuperBioChips Laboratories (CQ2 and CQN2; Seoul, South Korea). Formalin-fixed, paraffin-embedded GC tissues from 63 patients who received tumor resection at National Cheng Kung University Hospital (NCKUH) were acquired and used in conformity with Institutional Review Board-approved protocols (Table S1). Informed consent was obtained from all the patients. Tissue sections were deparaffinized, hydrated, immersed in citrate buffer for epitope retrieval in a microwave. The antibodies used are listed in Table S2 [20]. The staining was detected using the DAKO EnVision kit (Agilent Technologies, Santa Clara, CA, USA). All the IHC staining was evaluated by an expert pathologist (C.T. Chiang) and the staining intensities were quantified at the single-cell level with at least 300 tumor cells counted per tumor (3 tissue sections per tumor; at least 100 tumor cells counted per sections). IF staining of cells grown on culture plastics was performed using standard protocols. Confocal imaging was performed using a Nikon Digital Eclipse C1 confocal microscope system.

Cell culture and gene expression manipulations

AGS and NCI-N87 cells (American Type Culture Collection) were maintained as suggested by the provider. The

sustained knockdown (KD) of *ASPM* expression including all its putative transcript variants was achieved by lentivirus-mediated RNA interference (RNAi) using validated small hairpin RNA (shRNA) oligonucleotides in the lentivector pLKO.1-puro (TRCN0000118905 and SHC002V [non-target control]; Sigma-Aldrich, St. Louis, MO, USA). The specific KD of *ASPM* variant 1 (*ASPM*v1) expression, which encodes ASPMiI (NCBI RefSeq: NP_060606.3) was carried out by lentivirus-mediated transduction of small hairpin RNA (shRNA) using 2 independent RNAi target sequences (shRNA #4 and shRNA #3) specific for the exon 18 of the *ASPM* gene (unique to *ASPM*v1) and have been described previously [20]. The sustained KD of *FOXM1* expression was achieved by lentivirus-mediated RNA interference (TRCN0000015545 and TRCN0000015544, MISSION shRNA lentiviruses; Sigma-Aldrich). The lentivirus-mediated overexpression (OE) vectors of dishevelled 3 (*DVL3*) and *FOXM1* were purchased from Origene Technologies *Inc*. (Rockville, MD, USA). Lentivirus was produced as previously described [20].

IB and co-immunoprecipitation (IP)

IB and co-IP analyses were performed according to standard protocols as described previously [20]. Proteins were revealed after SDS/PAGE and immunoblotting with the indicated antibodies (Table S2).

qRT-PCR

qRT-PCR analysis was performed on the amplified RNA using the LightCycler FastStart DNA MASTERPLUS SYBR Green I Kit and the LightCycler System (Roche Diagnostics GmbH, Mannheim, Germany) according to the manufacturer's instructions. Oligonucleotide primers were designed using Primer Bank (http://pga.mgh.harvard.edu/primerbank/index.html).

Chromatin IP (ChIP)

ChIP experiments were carried out using primers specific for the putative binding sites (PBS) of FOXM1 on the promoter regions of *ASPM* as described previously [31]. Approximately 2–5 µL of ChIP-enriched chromatins was subjected to a standard qRT-PCR and the enrichment of specific genomic regions was assessed relative to either control IgG or the control cells.

Luciferase reporter assay

For luciferase reporter assay, cells were transduced with Cignal Lenti TCF/LEF Reporter (Qiagen, Venlo, The Netherlands) according to the manufacturer's protocol. Following stimulation of the cells with recombinant human WNT3A (250 ng/mL for 16 h; R&D Systems) or vehicle, the reporter activity was measured using the ONE-GloTM Luciferase Assay System (Promega, Madison, WI, USA).

Flow cytometry and tumorsphere assays

To analyze CSC populations by flow cytometry, cells were dissociated, antibody-labeled (1–2 µg per 10^6 cells × 1 h) and resuspended in HBSS/2% FBS as previously described [32, 33]. The antibodies used are listed in Table S2. The ALDEFLUOR assay (StemCell Technologies, Vancouver, BC, Canada) was performed according to the manufacturer's recommendation. Flow cytometry was done used a FACSCanto™ II flow cytometer (BD Biosciences, Franklin Lakes, NJ, US) with the electronic gating set according to cells stained with the corresponding isotype-matched control IgG. The tumorsphere assay and the limiting dilution assay (LDA) were performed as previously described [19, 34].

Animal models

GAC cells were lentivirally transduced a green fluorescence protein (GFP) and firefly luciferase (FF-Luc) fusion vector (UBC-EGFP-T2A-Luc; System Biosciences, CA, USA), and the GFP-positive cells were sorted. The cells were then infected with the lentivirus expressing the ASPM-specific shRNA or a non-target control as described above, after which the cells (1×10^6 cells) in 100 µl (1:1 Matrigel:cells) were inoculated into the flank of 8-week-old male NOD.CB17-*Prkdcscid*/NcrCrlBltw (NOD/SCID) mice (BioLASCO Taiwan, Taipei City, Taiwan) and tumor mass and distribution were assessed by bioluminescence imaging (BLI; the IVIS Imaging System, Caliper Life Sciences, Waltham, MA). For the peritoneal carcinomatosis model, FF-Luc-transduced GAC cells (1×10^6 cells) were injected directly into the peritoneal cavity of NOD/SCID mice. Protocols for animal care and experimentation were approved by the Institutional Animal Care and Use Committee of National Health Research Institutes (Zhunan, Miaoli County, Taiwan), and were adhered to the NIH Guide for the Care and Use of Laboratory Animals.

Statistical analysis

The statistical programming language R (cran.r-project.org) and SPSS 10.0 software (SPSS, Chicago, IL, USA) were used to conduct the statistical analysis of our data. Survival curves were generated using the Kaplan–Meier method. The curves were plotted and compared using the log-rank test using the Prism 6.01 software (GraphPad Software). A cut-off value that best discriminates between groups with respect to outcome was determined using the

Concordance Index, where an index of 1.0 is perfect discrimination [35]. The data from the LDA were analyzed and plotted using the ELDA software (http://bioinf.wehi.edu.au/software/elda/index.html).

Results

The transcript level of *ASPM* is upregulated in GC and correlates with poor patient prognosis

Previously, *Oncomine* analysis based on published GC transcriptome data sets has revealed a significant increase in the transcript level of *ASPM* in GC tissues compared with non-tumor tissues [21]. We confirmed in RNA sequencing data that the transcript level of *ASPM* significantly increased in GC tissues compared with that of normal tissues (Fig. 1a). Clinical correlative analyses conducted in several large patient cohort ($N=945$ in total) revealed that the tumors with a high transcript level of *ASPM* are associated with a significantly worse overall survival than those with a low level of *ASPM* (Fig. 1b). Moreover, the *ASPM* expression strongly correlates with the relapse-free survival of GC patients (Fig. 1c), implicating that ASPM is associated with the aggressive behavior of GC.

ASPM contributes to GC progression and aggressiveness

The upregulated expression of ASPM in GC tissues and its prognostic significance in GC patients raised the possibility of its potential oncogenic role in GC. We thus stably expressed an FF-Luc reporter in primary GC-derived AGS cells with *ASPM* KD or control KD and injected them subcutaneously into the flank of immunodeficient NOD/SCID mice. Remarkably, KD of *ASPM* expression almost abolished the tumorigenic potential of AGS cells (Fig. 1d). Likewise, advanced GC NCI-N87 cells deficient in *ASPM* expression failed to produce xenografted tumors in NOD/SCID mice (Fig. 1e).

Since advanced GC is frequently associated with peritoneal carcinomatosis, we injected NCI-N87-FF-Luc cells with *ASPM* KD or control KD into the peritoneal cavity. KD of *ASPM* expression abrogated more than 95% of the BLI signals emitted from the abdominal cavity compared with the control KD group (Fig. 1f). Thus, the mice bearing ASPM-KD GC cells developed a significantly less amount of peritoneal fluid than those mice with control-KD (data not shown). These data lend support to the important role of ASPM in GC progression and aggressiveness.

The expression of ASPMiI is prognostically important in GC

Whilst the preceding data support the importance of ASPM in GC, they did not distinguish among different protein isoforms of ASPM, which may play different roles in oncogenesis [20, 36]. To this end, we carried out TMA analysis of 59 GC tissues and the paired normal gastric epithelium for the staining of ASPMiI and ASPMiII using isoform-specific antibodies recently developed by our group. We found that ASPMiI is expressed mainly in the cytoplasm of a small subset ($\geq 2+$; ~10.1%) of normal gastric epithelial cells, especially those localized within the isthmus zone of the gastric oxyntic glands as previously described [21] (Fig. 2a, inset). By contrast, ASPMiII is expressed in both the cytoplasm and the nuclei of normal epithelial cells throughout the glands (Fig. 2a). Importantly, GC cells significantly upregulate the expression of ASPMiI with approximately one-third (~35.5%) of the tumor cells exhibiting $\geq 2+$ staining (Fig. 2b, left panels), whereas the expression of ASPMiII only marginally increased in GC cells (Fig. 2b, right panels). Notably, the expression of both ASPM isoforms exhibit a considerable cell-to-cell heterogeneity within the same tumors ($P<0.001$ by ANOVA). Of note, the above-mentioned expression pattern of ASPM isoforms is not restricted to the intestinal-type of GC and also applies to the diffuse-type of GC ($N=8$; Fig. S1). Using IF analysis, we confirmed the differential subcellular distributions of ASPMiI and ASPMiII in established GC cell lines AGS and NCI-N87 cells. Specifically, ASPMiI is predominantly expressed in the cytoplasm of GC cells, whereas ASPMiII is mainly nuclearly localized (Fig. 2c and data not shown).

Given that ASPMiI expression is specifically upregulated in GC tissues, we investigated its prognostic role by performing its IHC staining in the whole-tumor tissue sections from 63 patients with resected GC (Table S1). In light of the considerable cell-to-cell expressional heterogeneity of ASPMiI, we scored its staining intensity at the single-cell resolution and calculated the percentage of the tumor cells exhibiting a $\geq 2+$ staining intensity of ASPMiI for each tumor, which we denoted the "ASPMiI Positive Score (PS)". We found that the tumors exhibiting an ASPMiI PS of 10% or higher are associated with a significantly worse survival than those with a low ASPMiI PS (Fig. 2d). Furthermore, multivariable analysis confirmed that ASPMiI PS is a significant predictor of survival (Cox regression $P=0.043$) independent of standard clinicopathologic variables (Table S3), underscoring the important role of ASPMiI in GC progression.

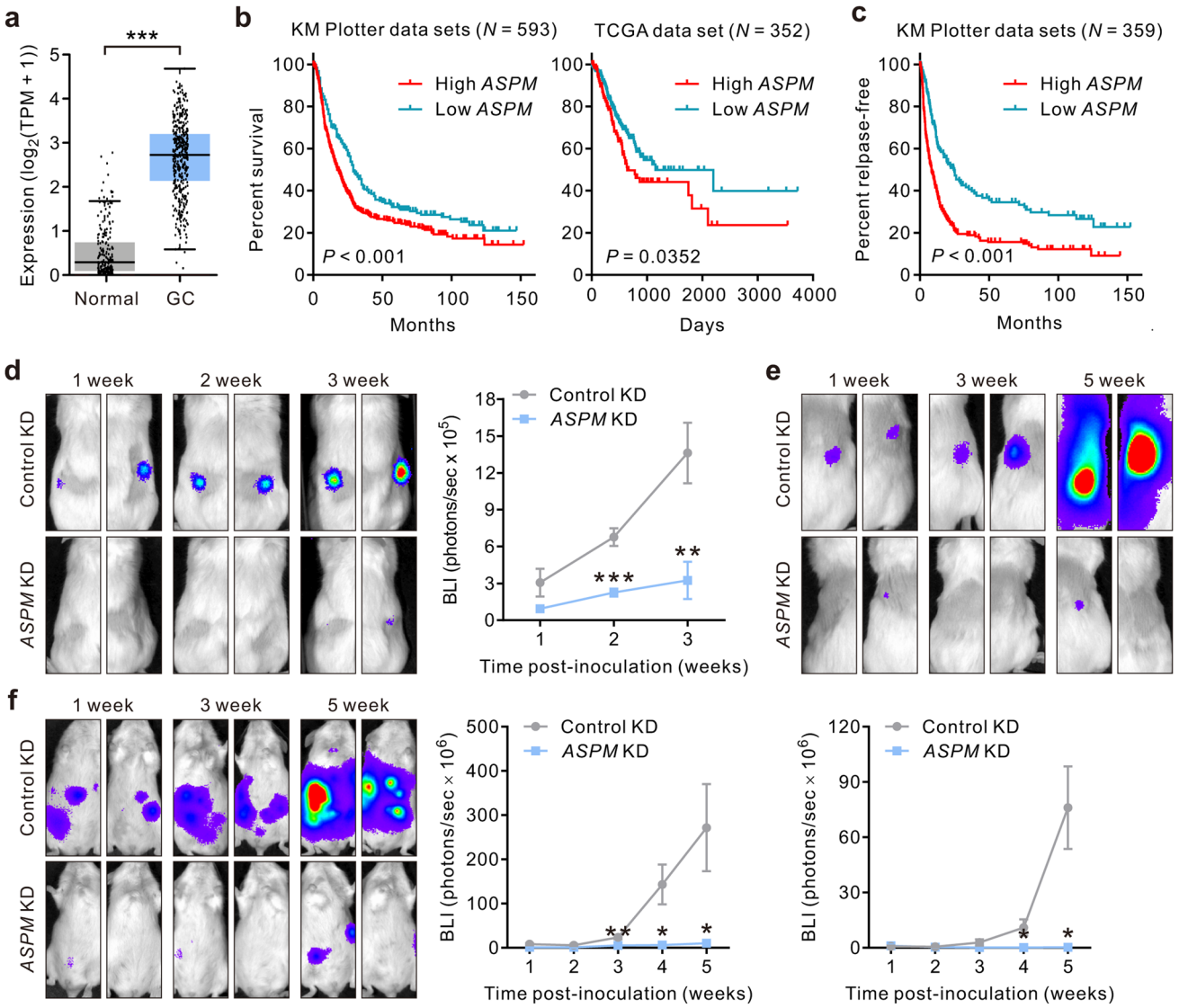

Fig. 1 ASPM expression relates to poor prognosis in GC and contributes to tumor progression. **a** Box plots of the expression level (transcripts per million, TPM) of *ASPM* in normal gastric tissue ($N=211$) and GC tissues ($N=408$) in the TCGA RNA sequencing data set. ***$P<0.001$, *t* test. Kaplan–Meier survival curve comparing overall survival (**b**) or relapse-free survival (**c**) of patients with GA in the KM Plotter data sets ($N=593$) or the TCGA data set ($N=352$) with their tumors having a high or low transcript level of *ASPM*. **d** Representative bioluminescence images (BLI) of the tumors formed by control-KD or *ASPM*-KD AGS cells in NOD/SCID mice at the indicated time after cell inoculation. Right, tumor bulk quantified as BLI normalized photon counts as a function of time (mean ± SEM, $N=6$ mice in each group). *$P<0.01$ compared with control KD, *t* test. **e** Representative BLI of the tumors formed by control-KD or *ASPM*-KD NCI-N87 cells in NOD/SCID mice. Bottom, tumor bulk quantified as BLI normalized photon counts (mean ± SEM, $N=6$ mice in each group). **$P<0.01$; ***$P<0.001$ compared with control KD, *t* test. **f** Representative BLI of the peritoneally injected NCI-N87 cells with control KD or *ASPM* KD. Right, the magnitude of tumor cell dissemination in the peritoneal cavity quantified as BLI normalized photon counts as a function of time (mean ± SEM, $N=6$ mice in each group). *$P<0.05$; **$P<0.01$ compared with control KD, *t* test

ASPMiI regulates the protein stabilities of DVL3 and β-catenin in GC cells

Recent studies have shown that ASPM, especially ASPMiI, augments canonical Wnt signaling in malignant cells [17, 18, 37]. We thus posited that ASPMiI also regulates Wnt activity in GC cells. Indeed, co-IF analysis on human GC tissues revealed that ASPMiI significantly colocalizes with active β-catenin in the cytoplasm of GC cells (Fig. 3a, b). To study the functional role of ASPMiI in Wnt signaling, we specifically down-regulated the expression of ASPMiI, but not ASPMiII, using lentivirus-mediated RNAi

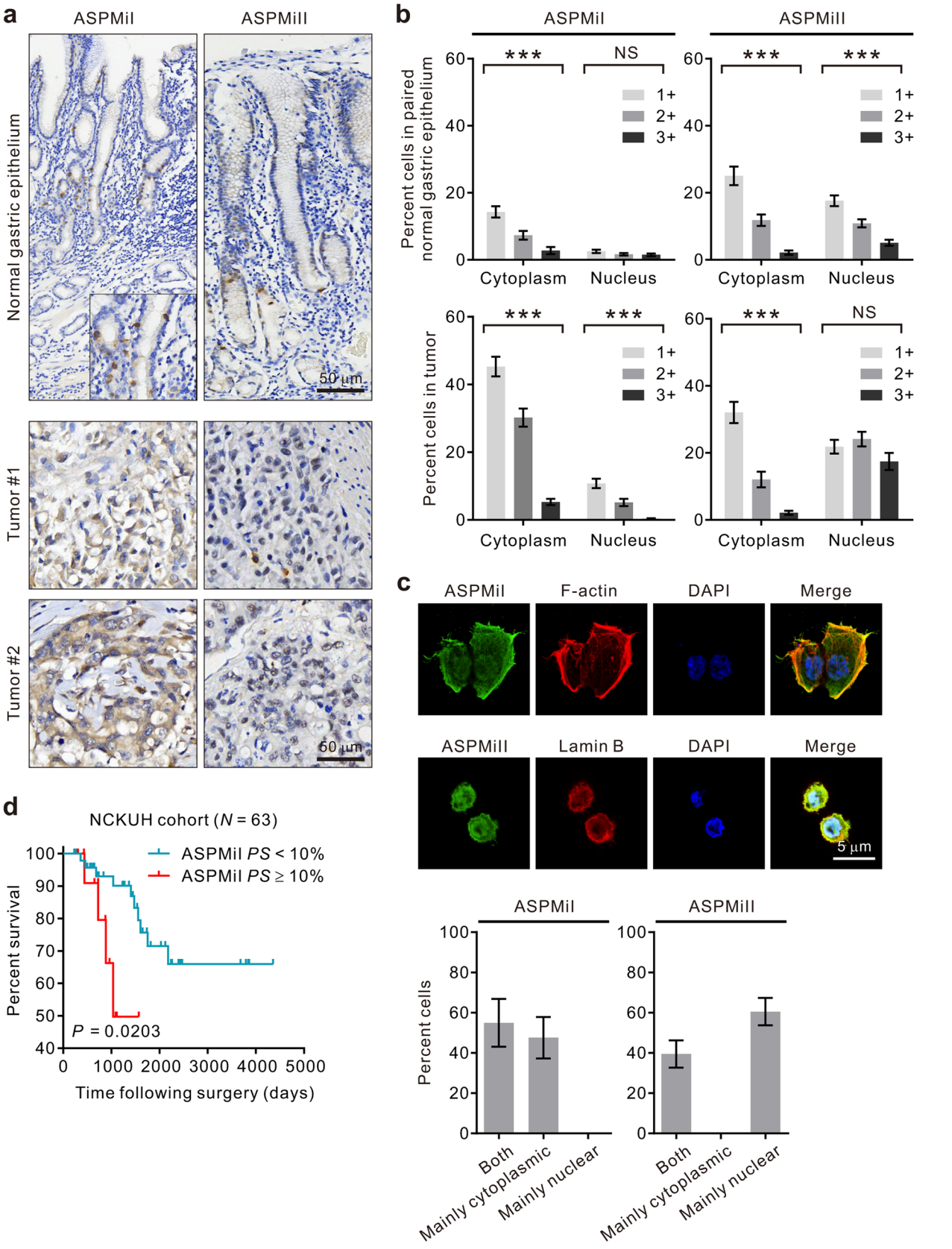
a
ASPMiI
ASPMiII
Normal gastric epithelium
Tumor #1
Tumor #2
50 μm
60 μm
b
ASPMiI
ASPMiII
Percent cells in paired normal gastric epithelium
Percent cells in tumor
***
NS
1+
2+
3+
Cytoplasm
Nucleus
c
ASPMiI
F-actin
DAPI
Merge
ASPMiII
Lamin B
5 μm
Percent cells
Both
Mainly cytoplasmic
Mainly nuclear
d
NCKUH cohort (N = 63)
ASPMiI PS < 10%
ASPMiI PS ≥ 10%
Percent survival
P = 0.0203
Time following surgery (days)

◂**Fig. 2** The expression patterns of ASPM isoforms in GC tissues and the prognostic role of ASPM isoform I (ASPMiI). **a** Representative IHC staining of ASPMiI and ASPMiII in human GC tissues and the adjacent normal gastric epithelium (×20 magnification). Inset, ASPMiI-positive-staining cells in the isthmus zone of normal gastric oxyntic glands. **b** Bar chart showing the staining intensities (1+ to 3+) of ASPMiI and ASPMiII in the GC and normal epithelial tissues in **a** (mean ± SEM, $N=59$). ***$P<0.001$; NS, not significant, one-way *ANOVA*. **c** Representative immunofluorescence (IF) images showing the subcellular localization of ASPMiI or ASPMiII (green) in AGS cells. Nuclei were counterstained with 4′,6-diamidino-2-phenylindole (DAPI; blue). Bottom, quantification of the subcellular localization of ASPMiI or ASPMiII (mean ± SEM, $N=4$). **d** Kaplan–Meier survival curve comparing overall survival of the patients in the NCKUH cohort stratified according to the ASPMiI Positive Score (PS). The cut-off value of the ASPMiI *PS* (10%) was determined using the Concordance Index

by transducing GC cells with two previously validated shRNAs (shRNA#3 and #4) targeting *ASPM*v1 (encoding ASPMiI) (Fig. 3c; Fig. S2a, b). Remarkably, the specific KD of *ASPM*v1 expression using *ASPM*v1-specific shRNA#4 and #3 both abolished the WNT3A-stimulated Wnt pathway activation in GC cells (Fig. 3d; Fig. S2c). Given that the ability of ASPM to augment Wnt activity has been attributed to its ability to stabilize the upstream Wnt regulator DVL proteins [17, 18], we examined their protein abundance levels in GC cells. We uncovered that down-regulating ASPMiI expression significantly reduced the level of DVL3 but not DVL1 or DVL2 (Fig. 3e; Fig. S2d). Indeed, a co-IP assay confirmed the strong interaction of ASPMiI with DVL3 (Fig. 3f). Consistently, KD of *ASPM*v1 expression enhanced the poly-ubiquitination of DVL3 and enhanced the recruitment of its specific E3 ligase Cullin 3 (Fig. 3g) [38]. Echoing these findings, the concurrent OE of *DVL3* could restore the Wnt pathway activity that had been reduced by KD of *ASPM*v1 expression (Fig. 3h), suggesting that ASPMiI regulates Wnt–β-catenin signaling by stabilizing the DVL3 protein in GC cells.

ASPMiI critically contributes to gastric cancer stemness

Malignant tumor cells frequently co-opt the Wnt-regulated self-renewal processes to acquire a stem-like phenotype to facilitate malignant progression [7]. The important functional role of ASPMiI in Wnt activity in GC cells motivated us to investigate its potential role in GC stemness. We thus measured the proportion of GC cells expressing cell-surface Leucine Rich Repeat Containing G Protein-Coupled Receptor 5 (LGR5) or aldehyde dehydrogenase 1 (ALDH1), which contain the enriched population of CSCs in GAC [39, 40]. KD of *ASPM*v1 expression using shRNA#4 or shRNA#3 significantly shrank the populations of $LGR5^+$ and $ALDH1^+$ cells compared with those with control KD in different GC lines (Fig. 4a; Fig. S2e, f), and substantially lowered the expression levels of the pluripotency- and stemness-associated genes, including *EZH2*, *KLF4*, *MYC*, *LGR5*, *NANOG*, *POU5F1*, *SMO*, and *SOX2*, in GC cells (Fig. 4b). Indeed, ASPMiI-deficient GC cells exhibited a considerably lower tumorsphere-forming ability, a functional surrogate of cancer stemness, than that of control cells (Fig. 4c). Corroborating these findings, co-IF analysis showed that ASPMiI significantly colocalizes with representative stemness markers LGR5 and SOX2 in human GC tissues (Fig. 4d, e). These results suggest that CSCs in GC may rely on ASPMiI to maintain their population as well as their tumorigenic potential.

FOXM1 augments Wnt activity and gastric cancer stemness by regulating ASPMiI and DVL3 expressions

Both FOXM1 and ASPM have been shown to regulate Wnt signaling [27, 28], which prompted us to investigate their potential interplay in GC cells. We first verified that *FOXM1* expression is significantly upregulated and strongly correlates with the transcript level of *ASPM*v1 in human GC tissues (Fig. 5a, b). Concordantly, co-IF and Venn diagram analyses confirmed that the subsets of CG cells staining positively (moderate to bright staining) for FOXM1, ASPMiI or DVL3 considerably overlaps with each other (Fig. 5c, d). In analogous to ASPM and ASPMiI, the expression level of *FOXM1* correlates with the poor prognosis in patients with GC (Fig. 5e).

To further substantiate the preceding clinical correlative analyses, we conducted a series of molecular studies and thereby established the crucial role of FOXM1 in the expressions of ASPMiI, DVL3, and β-catenin, the Wnt pathway activity, and the stemness properties of GC cells. First, we showed that KD of *FOXM1* expression diminished the expression of ASPMiI in GC cells (Fig. 5f). ChIP-qRT-PCR analysis revealed that FOXM1 strongly binds to the promoter of *ASPM* in GC cells (Fig. 5g). Consistently, KD of *FOXM1* expression substantially reduced the transcript level of *ASPM*v1 (Fig. 5h), suggesting that FOXM1 regulates *ASPM* expression at the transcriptional level. Moreover, affirming the findings previously reported in glioma and leukemia cells [27, 28], co-IP analysis revealed that FOXM1

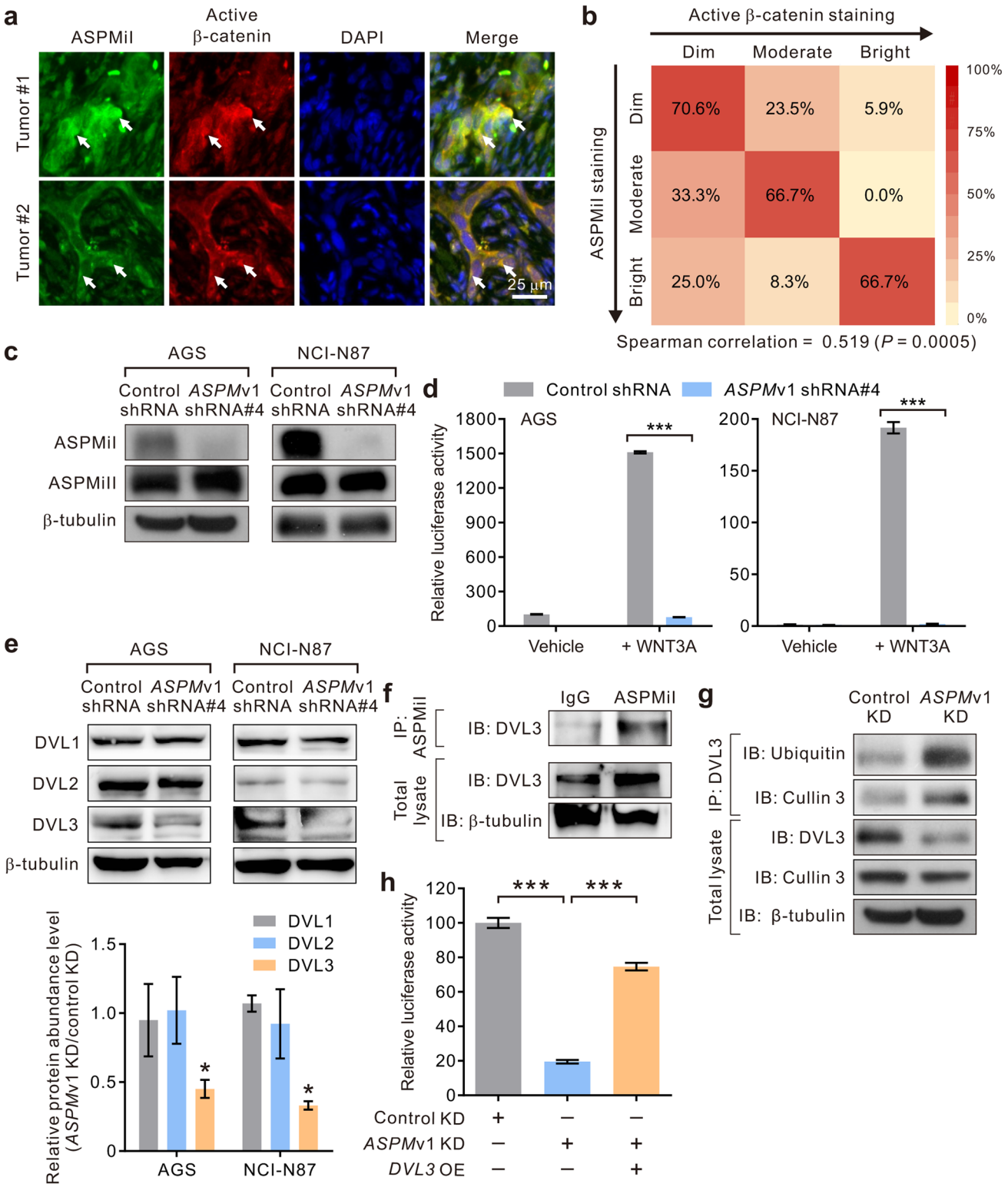
a
ASPMiI
Active β-catenin
DAPI
Merge
Tumor #1
Tumor #2
25 μm
b
Active β-catenin staining
Dim
Moderate
Bright
ASPMiI staining
70.6%
23.5%
5.9%
33.3%
66.7%
0.0%
25.0%
8.3%
66.7%
100%
75%
50%
25%
0%
Spearman correlation = 0.519 (P = 0.0005)
c
AGS
NCI-N87
Control shRNA
ASPMv1 shRNA#4
ASPMiI
ASPMiII
β-tubulin
d
Control shRNA
ASPMv1 shRNA#4
AGS
NCI-N87
Relative luciferase activity
***
Vehicle
+ WNT3A
e
AGS
NCI-N87
Control shRNA
ASPMv1 shRNA#4
DVL1
DVL2
DVL3
β-tubulin
Relative protein abundance level (ASPMv1 KD/control KD)
f
IgG
ASPMiI
IP: ASPMiI
IB: DVL3
Total lysate
IB: β-tubulin
g
Control KD
ASPMv1 KD
IP: DVL3
IB: Ubiquitin
IB: Cullin 3
Total lysate
IB: DVL3
IB: Cullin 3
IB: β-tubulin
h
Relative luciferase activity
Control KD
ASPMv1 KD
DVL3 OE

◂**Fig. 3** ASPMiI regulates Wnt pathway activity and DVL3 in GC cells. **a** Representative IF images showing the colocalization (yellow) of ASPMiI (green) with active β-catenin (red) in human GC tissues. Nuclei were counterstained with DAPI (blue). **b** Heatmaps illustrating the correlation of the staining intensity of ASPMiI with that of active β-catenin in GC tissues ($N=8$ tumors). **c** Immunoblotting (IB) analysis showing the effect of the specific KD of *ASPM*v1 expression using lentivirus-mediated transduction of *ASPM*v1 shRNA #4 in NCI-N87 cells, which specifically reduced the protein abundance level of ASPMiI but not ASPMiII. β-tubulin was included as a loading control. **d** Relative Wnt-specific luciferase activity in control- or *ASPM*v1-KD and WNT3A-treated NCI-N87 cells (mean ± SEM, $N=3$ biological replicates with two technical replicates). ***$P<0.001$, t test. **e** IB analysis of DVL1, DVL2 and DVL3 in control-KD or *ASPM*v1-KD NCI-N87 cells. β-tubulin was included as a loading control. Bottom, the fold of reduction in the protein abundance levels of DVL proteins (mean ± SEM, $N=3$). *$P<0.05$, t test. **f** Co-immunoprecipitation (IP) analysis showing that ASPMiI strongly associates with DVL3 in NCI-N87 cells. **g** IB analysis showing that KD of *ASPM*v1 expression increases the poly-ubiquitination of the immunoprecipitated DVL3 protein and enhanced the recruitment of the E3 ligase Cullin 3 to DVL3 in NCI-N87 cells. The cells were treated with the proteasome inhibitor MG-132 (10 μM for 12 h) before the collection of the protein lysate. **h** Lentivirus-mediated overexpression (OE) of *DVL3* restored the Wnt-specific luciferase activity in NCI-N87 cells with KD of *ASPM*v1 expression (mean ± SEM, $N=3$ biological replicates with two technical replicates). ***$P<0.001$, t test

strongly associated with β-catenin in GC cells (Fig. 5i). Furthermore, KD of *FOXM1* expression markedly lowered the protein abundance levels of DVL3 as well as β-catenin in GC cells (Fig. 5j) and reduced the population of CSCs (Fig. 5k) and inhibited their tumorsphere-forming ability (Fig. 5l).

ASPMiI is indispensable for FOXM1-mediated Wnt/β-catenin activation

The findings that FOXM1 can transcriptionally regulate the expression of ASPMiI as well as directly regulate β-catenin translocation and expression [27, 28] (Fig. S3) raise an interesting question as to their relative importance in the Wnt signaling transduction and activity in GC cells. Since KD of *ASPM*v1 expression almost completely abrogated the WNT3A-induced Wnt activation in GC cells (Fig. 3d) despite a high endogenous level of FOXM1 expression (data not shown), we surmised that ASPMiI-mediated DVL3 and β-catenin stabilization may be more important than the direct effect of FOXM1 on β-catenin. ASPM is a huge (~ 409 kDa) protein whose OE in cells is highly technically challenging as shown previously [18]. We thus sought to address the above possibility by overexpressing its downstream effector DVL3 in GC cells. Indeed, while KD of *FOXM1* expression markedly diminished β-catenin expression, the concurrent OE of *DVL3* was able to significantly restore the protein abundance level of β-catenin (Fig. 6a). Conversely, forced OE of *FOXM1* even at a super-physiological level failed to rescue the protein levels of β-catenin or DVL3 in ASPMiI-deficient GC cells (Fig. 6b). In accordance with these molecular studies, we confirmed at functional level that the concurrent OE of *FOXM1* could not restore the Wnt pathway activity (Fig. 6c) or the tumorsphere-forming capacity of GC cells deficient in ASPMiI expression (Fig. 6d). These data underscored the indispensable role of ASPMiI in the FOXM1-dependent regulation of β-catenin and Wnt signaling activity in GC cells.

Discussion

GC is a molecularly heterogeneous disease with marked phenotypic and genomic diversity. Recent advances in genomic analyses have led to the identification of novel molecular subtypes in GC [10, 41]. Of note, the molecular patterns identified from a developed tumor may only reflect the accumulative effect of the malignant transformation process without providing information reflecting the pathogenetic processes. The only biology-informed biomarkers currently used in the clinic are the analysis of HER2, PD-L1 and/or microsatellite instability, which guides the use of anti-HER-2 therapies and immune checkpoint inhibitors [4, 42, 43]. Unfortunately, these therapies only benefit a small subset of GC patients and additional biology-informed and clinically applicable analysis that can guide the use of next-generation rationale therapies remains an unmet clinical need.

GC develops Wnt dysregulations at multiple levels ranging from ligands, receptors, upstream regulators and β-catenin [10, 11]. Notably, these genetic lesions were discovered by genomic analysis on whole-tumor samples, which do not consider the potential intra-tumoral and cell-to-cell heterogeneity in Wnt signaling as reported in other types of solid cancers [44, 45]. We have recently discovered the novel Wnt co-regulator ASPM, especially its isoform I (ASPMiI), which displayed a high intra-tumoral heterogeneity in prostate, pancreatic and liver cancers [18–20]. We here extended our findings to GC by demonstrating the considerable cell-to-cell heterogeneity in ASPM expression and Wnt activity in human GC tissues. Using a series of molecular and functional studies, we uncovered the Wnt-regulatory function of ASPMiI in stem-like GC cells and the intriguing molecular crosstalk of ASPMiI with another important Wnt and stemness regulator, FOXM1.

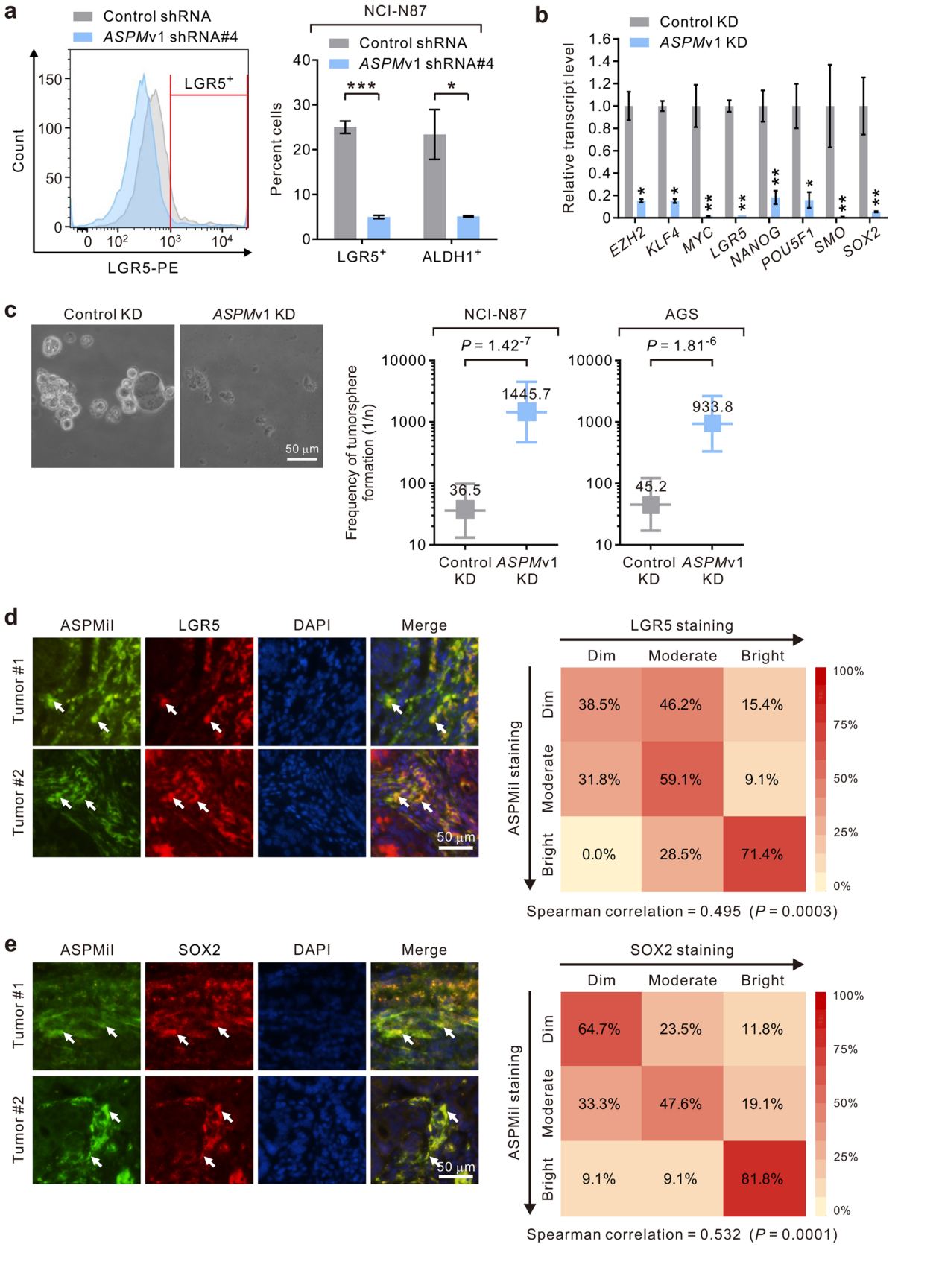
a
Control shRNA
ASPMv1 shRNA#4
LGR5+
Count
LGR5-PE
NCI-N87
Percent cells
LGR5+
ALDH1+
b
Control KD
ASPMv1 KD
Relative transcript level
EZH2
KLF4
MYC
LGR5
NANOG
POU5F1
SMO
SOX2
c
Control KD
ASPMv1 KD
50 μm
NCI-N87
AGS
P = 1.42-7
P = 1.81-6
Frequency of tumorsphere formation (1/n)
1445.7
36.5
933.8
45.2
d
ASPMil
LGR5
DAPI
Merge
Tumor #1
Tumor #2
LGR5 staining
Dim
Moderate
Bright
ASPMil staining
38.5%
46.2%
15.4%
31.8%
59.1%
9.1%
0.0%
28.5%
71.4%
Spearman correlation = 0.495 (P = 0.0003)
e
SOX2
SOX2 staining
64.7%
23.5%
11.8%
33.3%
47.6%
19.1%
9.1%
9.1%
81.8%
Spearman correlation = 0.532 (P = 0.0001)

◂**Fig. 4** ASPMiI regulates the stemness properties and the population of CSCs in GC cells. **a** Specific KD of *ASPM*v1 expression diminished the population of LGR5$^+$ or ALDH1$^+$ CSCs in NCI-N87 cells. Shown are representative flow cytometry plots showing pattern of LGR5 expression in control-KD or *ASPM*v1-KD NCI-N87 cells. Right, the percentage of LGR5$^+$ or ALDH1$^+$ NCI-N87 cells (mean ± SEM, $N=3$ biological replicates with two technical replicates). Statistical analysis was performed using unpaired *t* test. $^*P<0.05$, $^{***}P<0.001$, *t* test. **b** The transcript levels of the indicated pluripotency- and stemness-associated factors in *ASPM*v1-KD NCI-N87 cells compared with control-KD cells as measured by qRT-PCR (mean ± SEM, $N=3$ biological replicates with two technical replicates). $^*P<0.05$; $^{**}P<0.01$ compared with control KD, *t* test. **c** Representative phase contrast images of tumorspheres formed by control-KD or *ASPM*v1-KD NCI-N87 cells in serum-free and nonadherent culture plates for 10 days. Right, limiting dilatation assay demonstrating the tumorsphere-forming efficacy of NCI-N87 and AGS cells with control KD or *ASPM*v1 KD (maximum likelihood estimates with 95% confidence interval, $N=4$ biological replicates with two technical replicates). **d, e** Representative IF images showing the colocalization (yellow) of ASPMiI (green) with LGR5 (red; **d**) or SOX2 (red; **e**) in human GC tissues. Nuclei were counterstained with DAPI (blue). Right panels, heatmaps illustrating the correlation of the staining intensity of ASPMiI with that of LGR5 (**d**) or SOX2 (**e**) in GC tissues ($N=8$ tumors). Nuclei were counterstained with DAPI (blue)

Importantly, we elucidated that FOXM1 regulates the stability of β-catenin, Wnt pathway activity and cancer stemness in GC cells in an ASPMiI-dependent manner. Our findings thus shed new lights on the molecular basis of the dysregulated Wnt signaling in GC cells and underscore the critical and indespensable role of the FOXM1/ASPMiI/β-catenin interplay in the Wnt pathway activity and the aggressiveness of GC.

The molecular mechanism by which ASPM augments Wnt signaling in cancer cells has been attributed to its ability to interact with selective DVL proteins, whereby inhibits their proteasome-dependent degradation [17, 18, 20]. Notably, we have recently mapped the region of ASPM that mediates its interaction with DVL, which is located within the region encoded by exon-18 (data not shown) and is missing in another major isoform of ASPM, ASPMiII [12, 20]. Consistently, we showed that the expression of ASPMiI is specifically upregulated in GC tissues, where it colocalizes with active β-catenin in the cytoplasm of cancer cells. By contrast, ASPMiII is expressed mainly in the nuclei of both normal epithelial cells and cancer cells (Fig. 2b). Notably, the differential subcellular distribution of ASPMiI and ASPMiII is not only mechanistically important but also prognostically significant. Whist a previous analysis interrogating into whole-tumor transcriptome datasets has demonstrated a potential poor prognostic role of ASPM in GC [21], this study did not distinguish among the transcript variants of *ASPM*. With the advent of novel isoform-specific antibodies, our study provides an unprecedented opportunity of elucidating the prognostic role of ASPM in GC in an isoform-specific manner. We showed that the protein abundance level of ASPMiI is upregulated mainly in the cytoplasm in approximately a third of GC tissues, which correlated that of active β-catenin and with the poor prognosis in patients with GC, whereas the expression level of ASPMiII did not. We thus envisage that the IHC staining of ASPMiI may serve to identify a novel subset of GC cells in the tumors or a subset of GC tumors that are Wnt active and may respond to various Wnt-targeted molecular therapeutics currently undergoing preclinical or clinical developments [46], potentially yielding novel therapeutic opportunity for advanced GC.

Whilst the expression of ASPM is found to be upregulated in a wide variety of human malignant tumors [13–16], the mechanisms giving rise to its elevated expression remain poorly understood. Also elusive are the molecular mechanisms underlying the elevated expression of ASPM in CSCs. The strong regulatory role of FOXM1 on the transcript level of *ASPM* in GC cells as identified in the present study may provide a plausible explanation as FOXM1 is known to be involved in development, regeneration, tumorigenesis, and its expression is upregulated in stem cells [27, 28]. Our rigorous molecular studies indicate that FOXM1 and ASPM work in concert to promote the stability of β-catenin, resulting in the activation of Wnt signaling as well as the stemness properties of GC cells. FOXM1 and the ASPMiI–DVL3 signaling axis converge on β-catenin through protein–protein interactions, wherein ASPMiI plays a crucial and indispensable role in this novel Wnt-regulatory module in CSCs (Fig. 7). Notably, our bioinformatics analysis revealed that many malignant tumors concurrently upregulate the expressions of FOXM1 and ASPM (data not shown), raising a compelling question as to whether the interplay between FOXM1, ASPM and β-catenin may also play an important role in Wnt activation and cancer stemness in other types of malignant tumors. Further studies are warranted to confirm the generality of the role of this novel oncogenic mechanism.

In conclusion, our findings illuminate a novel Wnt-related pathomechanism giving rise to and sustaining GC stemness and aggressiveness. We elucidate the interplay and the epistatic relationship among ASPMiI, FOXM1,

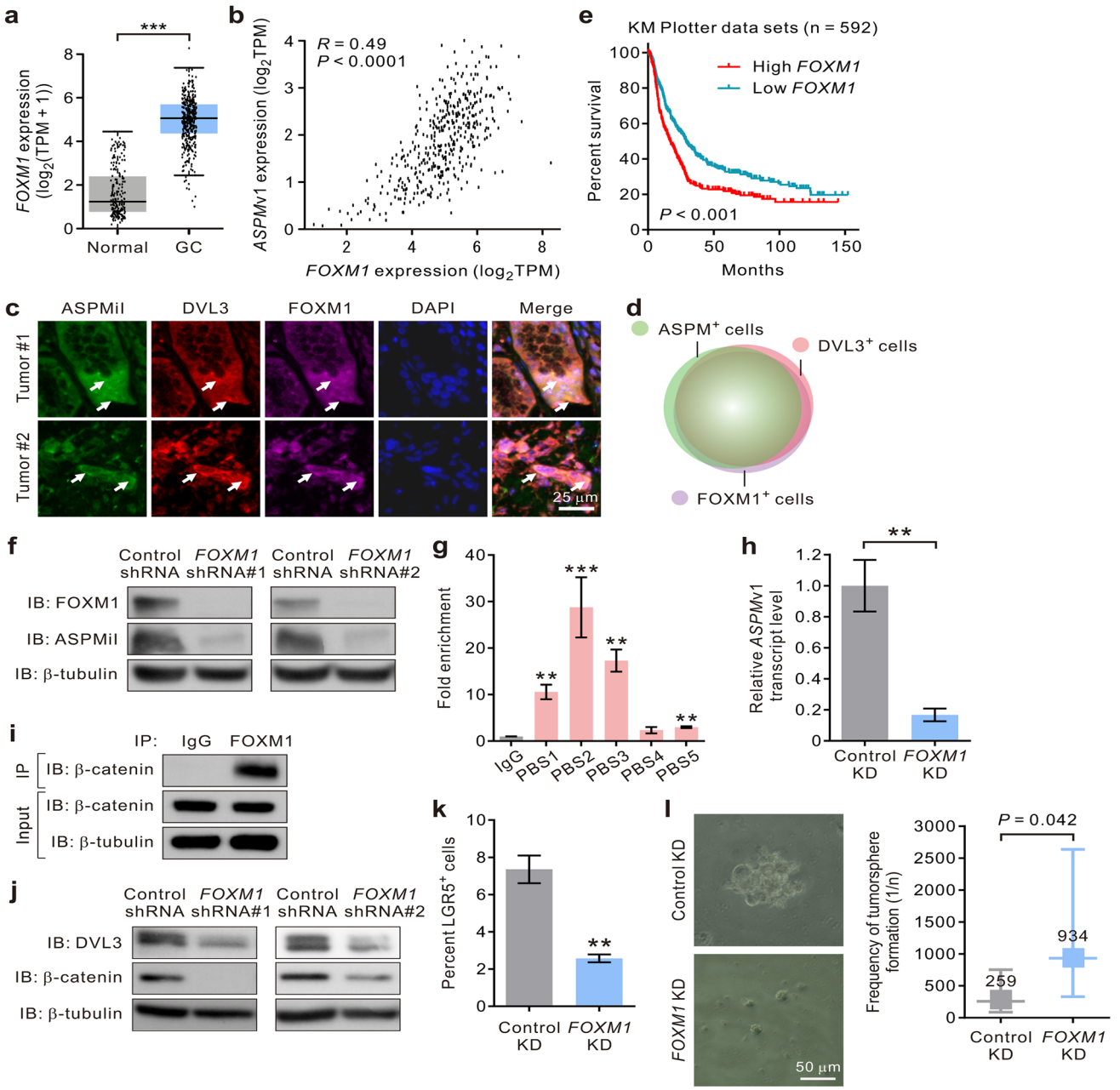

Fig. 5 The roles of FOXM1 in ASPM expression, Wnt activity, and cancer stemness in GC. **a** Box plots of the expression level (transcripts per million, TPM) of *FOXM1* in normal gastric epithelial tissue ($N=211$) and GC tissues ($N=408$) in the TCGA RNA sequencing data set. $^{***}P<0.001$, *t* test. **b** Scatter plot showing the correlation between the transcript levels of *ASPM*v1 and *FOXM1* in the TCGA RNA sequencing data set. **c** Representative IF images showing the colocalization of ASPMiI (green) with DVL3 (red) and FOXM1 (magenta) in human GC tissues. Nuclei were counterstained with DAPI (blue). **d** Venn diagram illustrating the overlap of the cell subsets stained positive for ASPMiI, DVL3, and FOXM1 in GC tissues ($N=8$ tissues). **e** Kaplan–Meier survival curve comparing overall survival of GC patients in the KM Plotter data sets ($N=592$) with their tumors having a high or low transcript level of *FOXM1*. **f** IB analysis showing the effect of KD of *FOXM1* expression using two different shRNAs on the protein abundance levels of FOXM1 and ASPMiI in NCI-N87 cells. β-tubulin was included as a loading control. **g** Chromatin immunoprecipitation (ChIP)-qRT-PCR assays showing that FOXM1 is recruited to several putative binding sites (PBS) on the *ASPM* promoter in NCI-N87 cells (mean ± SEM; $N=3$). $^{**}P<0.01$, $^{***}P<0.001$, *t* test. **h** KD of *FOXM1* expression reduced the transcript level of *ASPM*v1 in NCI-N87 cells as measured by qRT-PCR (mean ± SEM, $N=3$ biological replicates with two technical replicates). $^{**}P<0.05$ compared with control KD, *t* test. **i** Co-IP analysis showing that FOXM1 associates with β-catenin in NCI-N87 cells. **j** KD of *FOXM1* expression reduced the protein abundance levels of DVL3 and β-catenin in NCI-N87 cells. **k** KD of *FOXM1* expression reduced the population of $LGR5^+$ CSCs in NCI-N87 cells (mean ± SEM, $N=3$ biological replicates with two technical replicates). $^{**}P<0.01$, *t* test. **l** Tumorsphere assay and LDA demonstrating the tumorsphere-forming efficacy of control-KD or *FOXM1*-KD NCI-N87 cells (maximum likelihood estimates with 95% confidence interval, $N=4$ biological replicates with two technical replicates)

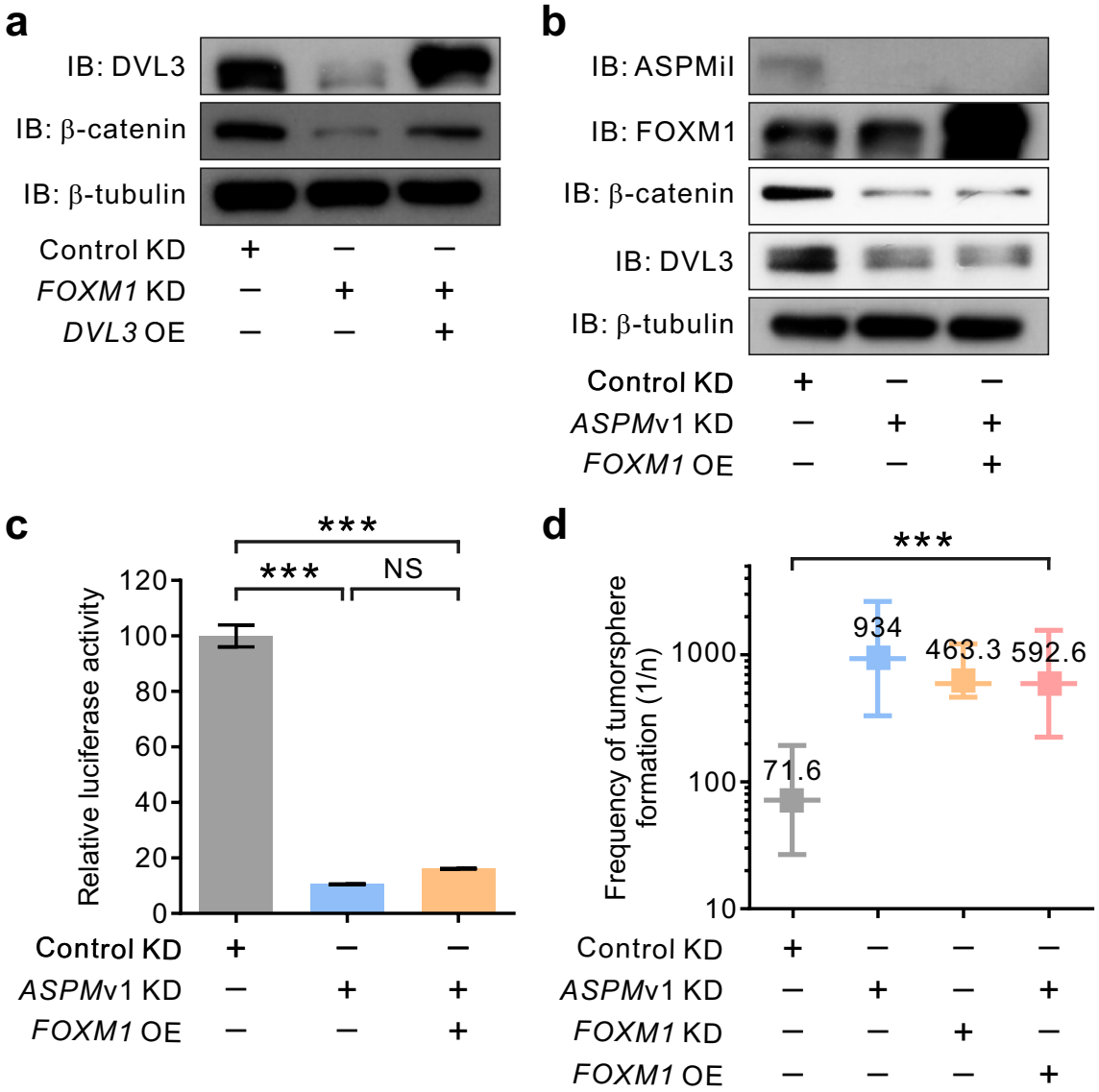

Fig. 6 FOXM1-mediated β-catenin/Wnt activation and GC stemness requires ASPMiI. **a** IB analysis showing that OE of *DVL3* significantly restored the protein abundance level of β-catenin in FOXM1-deficient NCI-N87 cells. **b** OE of *FOXM1* failed to rescue the protein abundance levels of β-catenin and DVL3 in ASPMiI-deficient NCI-N87 cells. **c** Wnt-specific luciferase activity in NCI-N87 cells with OE of *FOXM1* with or without the concurrent KD of *ASPM*v1 expression (mean ± SEM, $N = 3$ biological replicates with two technical replicates). ***$P < 0.001$, *t* test. NS, not significant. **d** LDA demonstrating the tumorsphere-forming efficacy of NCI-N87 cells with control KD, *ASPM*v1 KD or *FOXM1* KD with or without the concurrent OE of *FOXM1* (maximum likelihood estimates with 95% confidence interval, $N = 4$ biological replicates with two technical replicates)

DVL3, and β-catenin, which augments Wnt activity in CSCs in a cooperative manner. Our data not only highlight a promising role of ASPMiI and FOXM1 in the diagnosis of a novel Wnt-activated and stemness-high subtype of GC but also provides key molecular hubs toward which Wnt- and/or CSC-targeted rational therapies can be developed.

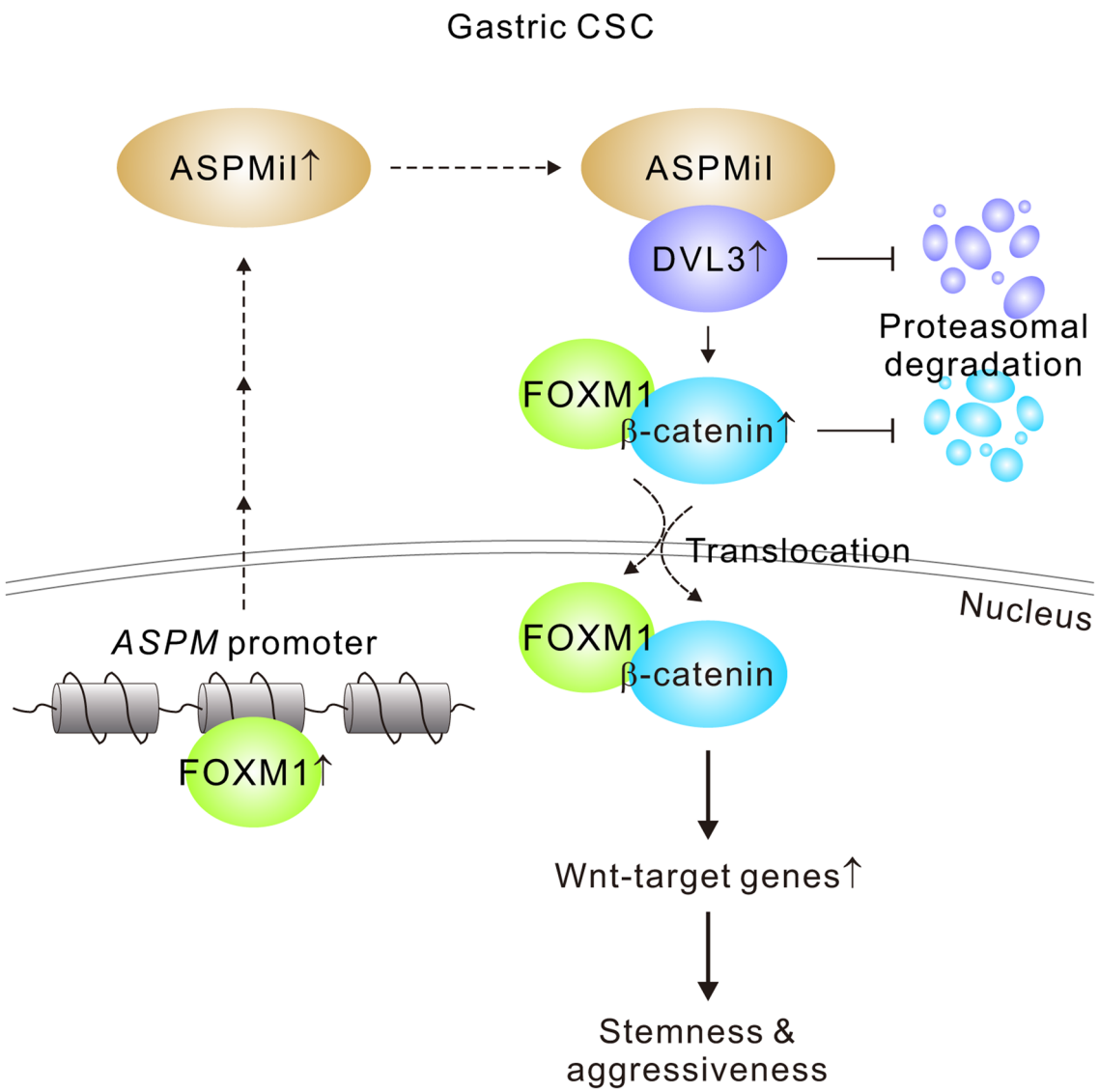

Fig. 7 Model depicting the FOXM1/ASPMiI/DVL3/β-catenin regulatory module that reinforces Wnt signals to control GC stemness and aggressiveness. CSCs in GC express a high level of FOXM1, which induces the transcription of *ASPM*. The ASPMiI protein specifically interacts with DVL3 in the cytosol and prevents it from the proteasome-dependent degradation, thereby stabilizing the β-catenin protein. In parallel, FOXM1 also directly mediates the nuclear translocation of β-catenin. This multi-mode regulatory module promotes β-catenin-dependent Wnt pathway activation, cancer stemness and aggressiveness in GC

Supplementary Information The online version contains supplementary material available at https://doi.org/10.1007/s10120-020-01154-5.

Acknowledgements This work was supported in part by Ministry of Science and Technology, Taiwan (MOST 108-2314-B-038-105, and MOST-109-2314-B-038-130 to K.K.T.), and Taipei Medical University (109-TMU-WFH-05, and DP2-107-21121-C-04 to K.K. T.), Wan Fang Hospital (109-WF-PHD-01 to Po-Jui Huang), Wan Fang Hospital, Chi-Mei Medical Center, and Hualien Tzu-Chi Hospital Joint Cancer Center Grant, Ministry of Health and Welfare (MOHW109-TDU-B-212-124020 to K.K.T.), and TMU Research Center of Cancer Translational Medicine" from The Featured Areas Research Center Program within the framework of the Higher Education Sprout Project by the Ministry of Education in Taiwan (K.K.T.).

Author contributions All of the listed authors contributed to the current study. CH, WL, KC, LC and TL conducted molecular and biochemical experiments; WL and KC performed animal studies; TC, PH, and YS performed collection of the tissue specimens, CC analyzed immunostaining; TC and PH compiled clinical data and performed statistical analysis; and KT supervised the research and prepared the manuscript. All authors have read and approved the final version of the manuscript.

Compliance with ethical standards

Conflict of interest The authors declare no potential conflict that is relevant to the manuscript.

References

1. Ferlay J, Soerjomataram I, Dikshit R, Eser S, Mathers C, Rebelo M, et al. Cancer incidence and mortality worldwide: sources, methods and major patterns in GLOBOCAN 2012. Int J Cancer. 2015;136(5):E359–86.
2. Wilke H, Muro K, Van Cutsem E, Oh SC, Bodoky G, Shimada Y, et al. Ramucirumab plus paclitaxel versus placebo plus paclitaxel in patients with previously treated advanced gastric or gastro-oesophageal junction adenocarcinoma (RAINBOW): a double-blind, randomised phase 3 trial. Lancet Oncol. 2014;15(11):1224–35.
3. Muro K, Chung HC, Shankaran V, Geva R, Catenacci D, Gupta S, et al. Pembrolizumab for patients with PD-L1-positive advanced gastric cancer (KEYNOTE-012): a multicentre, open-label, phase 1b trial. Lancet Oncol. 2016;17(6):717–26.
4. Kang YK, Boku N, Satoh T, Ryu MH, Chao Y, Kato K, et al. Nivolumab in patients with advanced gastric or gastro-oesophageal junction cancer refractory to, or intolerant of, at least two previous chemotherapy regimens (ONO-4538-12, ATTRACTION-2): a randomised, double-blind, placebo-controlled, phase 3 trial. Lancet. 2017;390(10111):2461–71.
5. Le DT, Durham JN, Smith KN, Wang H, Bartlett BR, Aulakh LK, et al. Mismatch repair deficiency predicts response of solid tumors to PD-1 blockade. Science. 2017;357(6349):409–13.
6. Reya T, Clevers H. Wnt signalling in stem cells and cancer. Nature. 2005;434(7035):843–50.
7. Malanchi I, Peinado H, Kassen D, Hussenet T, Metzger D, Chambon P, et al. Cutaneous cancer stem cell maintenance is dependent on beta-catenin signalling. Nature. 2008;452(7187):650–3.
8. Li Y, Welm B, Podsypanina K, Huang S, Chamorro M, Zhang X, et al. Evidence that transgenes encoding components of the Wnt signaling pathway preferentially induce mammary cancers from progenitor cells. Proc Natl Acad Sci USA. 2003;100(26):15853–8.
9. Heiser PW, Cano DA, Landsman L, Kim GE, Kench JG, Klimstra DS, et al. Stabilization of beta-catenin induces pancreas tumor formation. Gastroenterology. 2008;135(4):1288–300.
10. Wang K, Yuen ST, Xu J, Lee SP, Yan HH, Shi ST, et al. Whole-genome sequencing and comprehensive molecular profiling identify new driver mutations in gastric cancer. Nat Genet. 2014;46(6):573–82.
11. Flanagan DJ, Vincan E, Phesse TJ. Winding back Wnt signalling: potential therapeutic targets for treating gastric cancers. Br J Pharmacol. 2017;174(24):4666–83.
12. Kouprina N, Pavlicek A, Collins NK, Nakano M, Noskov VN, Ohzeki J, et al. The microcephaly ASPM gene is expressed in proliferating tissues and encodes for a mitotic spindle protein. Hum Mol Genet. 2005;14(15):2155–65.
13. Bruning-Richardson A, Bond J, Alsiary R, Richardson J, Cairns DA, McCormack L, et al. ASPM and microcephalin expression in epithelial ovarian cancer correlates with tumour grade and survival. Br J Cancer. 2011;104(10):1602–10.
14. Bikeye SN, Colin C, Marie Y, Vampouille R, Ravassard P, Rousseau A, et al. ASPM-associated stem cell proliferation is involved in malignant progression of gliomas and constitutes an attractive therapeutic target. Cancer Cell Int. 2010;10:1.
15. Lin SY, Pan HW, Liu SH, Jeng YM, Hu FC, Peng SY, et al. ASPM is a novel marker for vascular invasion, early recurrence, and poor prognosis of hepatocellular carcinoma. Clin Cancer Res. 2008;14(15):4814–20.
16. Xu Z, Zhang Q, Luh F, Jin B, Liu X. Overexpression of the ASPM gene is associated with aggressiveness and poor outcome in bladder cancer. Oncol Lett. 2019;17(2):1865–76.
17. Wang WY, Hsu CC, Wang TY, Li CR, Hou YC, Chu JM, et al. A gene expression signature of epithelial tubulogenesis and a role for ASPM in pancreatic tumor progression. Gastroenterology. 2013;145(5):1110–20.
18. Pai VC, Hsu CC, Chan TS, Liao WY, Chuu CP, Chen WY, et al. ASPM promotes prostate cancer stemness and progression by augmenting Wnt-Dvl-3-beta-catenin signaling. Oncogene. 2019;38:1340–53.
19. Liao WY, Hsu CC, Chan TS, Yen CJ, Chen WY, Pan HW, et al. Dishevelled 1-regulated superpotent cancer stem cells mediate Wnt heterogeneity and tumor progression in hepatocellular carcinoma. Stem Cell Rep. 2020;14(3):462–77.
20. Hsu CC, Liao WY, Chan TS, Chen WY, Lee CT, Shan YS, et al. The differential distributions of ASPM isoforms and their roles in Wnt signaling, cell cycle progression, and pancreatic cancer prognosis. J Pathol. 2019;249(4):498–508.
21. Vange P, Bruland T, Beisvag V, Erlandsen SE, Flatberg A, Doseth B, et al. Genome-wide analysis of the oxyntic proliferative isthmus zone reveals ASPM as a possible gastric stem/progenitor cell marker over-expressed in cancer. J Pathol. 2015;237(4):447–59.
22. Borhani S, Gartel AL. FOXM1: a potential therapeutic target in human solid cancers. Expert Opin Ther Targets. 2020;24(3):205–17.
23. Clark KL, Halay ED, Lai E, Burley SK. Co-crystal structure of the HNF-3/fork head DNA-recognition motif resembles histone H5. Nature. 1993;364(6436):412–20.
24. Kalin TV, Ustiyan V, Kalinichenko VV. Multiple faces of FoxM1 transcription factor: lessons from transgenic mouse models. Cell Cycle. 2011;10(3):396–405.
25. Kalinichenko VV, Major ML, Wang X, Petrovic V, Kuechle J, Yoder HM, et al. Foxm1b transcription factor is essential for development of hepatocellular carcinomas and is negatively regulated by the p19ARF tumor suppressor. Genes Dev. 2004;18(7):830–50.
26. Laoukili J, Kooistra MR, Bras A, Kauw J, Kerkhoven RM, Morrison A, et al. FoxM1 is required for execution of the mitotic programme and chromosome stability. Nat Cell Biol. 2005;7(2):126–36.
27. Zhang N, Wei P, Gong A, Chiu WT, Lee HT, Colman H, et al. FoxM1 promotes beta-catenin nuclear localization and controls Wnt target-gene expression and glioma tumorigenesis. Cancer Cell. 2011;20(4):427–42.
28. Sheng Y, Yu C, Liu Y, Hu C, Ma R, Lu X, et al. FOXM1 regulates leukemia stem cell quiescence and survival in MLL-rearranged AML. Nat Commun. 2020;11(1):928.
29. Quan M, Wang P, Cui J, Gao Y, Xie K. The roles of FOXM1 in pancreatic stem cells and carcinogenesis. Mol Cancer. 2013;12:159.
30. Li X, Qiu W, Liu B, Yao R, Liu S, Yao Y, et al. Forkhead box transcription factor 1 expression in gastric cancer: FOXM1 is a poor prognostic factor and mediates resistance to docetaxel. J Transl Med. 2013;11:204.
31. Zeng WJ, Cheng Q, Wen ZP, Wang JY, Chen YH, Zhao J, et al. Aberrant ASPM expression mediated by transcriptional regulation of FoxM1 promotes the progression of gliomas. J Cell Mol Med. 2020;24(17):9613–26.
32. Al-Hajj M, Wicha MS, Benito-Hernandez A, Morrison SJ, Clarke MF. Prospective identification of tumorigenic breast cancer cells. Proc Natl Acad Sci USA. 2003;100(7):3983–8.

33. Li C, Heidt DG, Dalerba P, Burant CF, Zhang L, Adsay V, et al. Identification of pancreatic cancer stem cells. Cancer Res. 2007;67(3):1030–7.
34. Arensman MD, Kovochich AN, Kulikauskas RM, Lay AR, Yang PT, Li X, et al. WNT7B mediates autocrine Wnt/beta-catenin signaling and anchorage-independent growth in pancreatic adenocarcinoma. Oncogene. 2014;33(7):899–908.
35. Pencina MJ, D'Agostino RB. Overall C as a measure of discrimination in survival analysis: model specific population value and confidence interval estimation. Stat Med. 2004;23(13):2109–23.
36. Timaner M, Shaked Y. Elucidating the roles of ASPM isoforms reveals a novel prognostic marker for pancreatic cancer. J Pathol. 2020;250(2):123–5.
37. Buchman JJ, Durak O, Tsai LH. ASPM regulates Wnt signaling pathway activity in the developing brain. Genes Dev. 2011;25(18):1909–14.
38. Jin X, Jeon HM, Jin X, Kim EJ, Yin J, Jeon HY, et al. The ID1-CULLIN3 axis regulates intracellular SHH and WNT signaling in glioblastoma stem cells. Cell Rep. 2016;16(6):1629–41.
39. Nguyen PH, Giraud J, Chambonnier L, Dubus P, Wittkop L, Belleannee G, et al. Characterization of biomarkers of tumorigenic and chemoresistant cancer stem cells in human gastric carcinoma. Clin Cancer Res. 2017;23(6):1586–97.
40. Barker N, Huch M, Kujala P, van de Wetering M, Snippert HJ, van Es JH, et al. Lgr5(+ve) stem cells drive self-renewal in the stomach and build long-lived gastric units in vitro. Cell Stem Cell. 2010;6(1):25–36.
41. Cristescu R, Lee J, Nebozhyn M, Kim KM, Ting JC, Wong SS, et al. Molecular analysis of gastric cancer identifies subtypes associated with distinct clinical outcomes. Nat Med. 2015;21(5):449–56.
42. Bang YJ, Van Cutsem E, Feyereislova A, Chung HC, Shen L, Sawaki A, et al. Trastuzumab in combination with chemotherapy versus chemotherapy alone for treatment of HER2-positive advanced gastric or gastro-oesophageal junction cancer (ToGA): a phase 3, open-label, randomised controlled trial. Lancet. 2010;376(9742):687–97.
43. Kim ST, Cristescu R, Bass AJ, Kim KM, Odegaard JI, Kim K, et al. Comprehensive molecular characterization of clinical responses to PD-1 inhibition in metastatic gastric cancer. Nat Med. 2018;24(9):1449–58.
44. Cleary AS, Leonard TL, Gestl SA, Gunther EJ. Tumour cell heterogeneity maintained by cooperating subclones in Wnt-driven mammary cancers. Nature. 2014;508(7494):113–7.
45. Vermeulen L, De Sousa EMF, van der Heijden M, Cameron K, de Jong JH, Borovski T, et al. Wnt activity defines colon cancer stem cells and is regulated by the microenvironment. Nat Cell Biol. 2010;12(5):468–76.
46. Anastas JN, Moon RT. WNT signalling pathways as therapeutic targets in cancer. Nat Rev Cancer. 2013;13(1):11–26.